

INVESTIGATION OF IRREVERSIBLE REACTIVE LIQUID CHROMATOGRAPHY CONSIDERING LINEAR GENERAL RATE MODEL

by

Nadia KIRAN^b, Seemab BASHIR^{a*}, and Shamsul QAMAR^b

^aDepartment of Mathematics, AIR University, Islamabad, Pakistan

^bDepartment of Mathematics, COMSATS University Islamabad, Islamabad, Pakistan

Original scientific paper

<https://doi.org/10.2298/TSCI190705364K>

A two-component model of reactive liquid chromatography is presented considering $M \rightarrow N$ type reaction. The model incorporates surface and pore diffusions in the adsorbates, axial dispersion, interfacial mass transfer, first order chemical reactions in the liquid and particle phases, and two sets of boundary conditions. The model contains a system of four coupled PDE describing the dynamics of reactants and products in both phases. The Laplace transformation and eigen-decomposition technique are jointly applied to solve the model equations analytically. An efficient and accurate numerical Laplace inversion technique is utilized to retrieve back solutions in the original time domain. The developed semi-analytical results are verified against the numerical results of a high resolution finite volume scheme. A good agreement between the solutions not only confirms the accuracy of semi-analytical results but also validates the accuracy of proposed numerical scheme. This study extends and generalizes our previous analysis on heterogeneous reactions in the liquid chromatography. In order to analyze the behavior of a chromatographic reactor, different case studies are presented showing the effects of model parameters on the process.

Key words: *chromatographic reactor, analytical solutions, linear adsorption, liquid and solid phases reactions, mass transfer and reaction kinetics*

Introduction

High performance liquid chromatography (HPLC) is a popular chromatographic method that is typically designed in accordance to the structure of the stationary and mobile phases. This technique, which utilizes different adsorption affinities of the mixture components in their separation, identification and quantification, has gained a considerable popularity in the field of chemical engineering [1-4].

Amongst the all transport models of chromatography, the general rate model (GRM) is viewed as the most far-reaching model [2]. This model incorporates the transport mechanisms like advection, axial dispersion, diffusion through an external film surrounding the sorbent particles, and intraparticle diffusion in the stagnant mobile phase within the particle pores [1, 2, 5-7]. The model is sufficiently accurate for most of the chromatographic separations.

In the chemical industries, only the chemical reactions characteristically do not provide the desired results and that separation techniques are always demanded. Therefore, a wide

* Corresponding author, e-mail: sabbasi354736@yahoo.com

range of practical efforts have been made to combine these two processes into a single apparatus. Such type of apparatus is also used in the reactive chromatography, where both processes are merged together in a single chromatographic column [8-11]. The process has not only enhanced the conversion of reactants into products but has also produced high purity products and, thus, has got attention of several scientists in the past [1, 9].

Homogeneous and heterogeneous catalyzed chemical reactions are available inside this integrated process. In a homogeneous reaction, the catalyst is present in the same phase of the reactants, *i. e.* in the liquid phase. Whereas, in the heterogeneous reactions, the sorbent particles play the role of catalyst for the chemical reaction [8]. In the reactive chromatography, the chromatographic column behaves as a reactor itself. The pulses of reactants are periodically injected to the reactor which convert into products. During their propagation through the column, products separation occur. If the strongly adsorbed reactant produces weakly adsorbed product or weakly adsorbed reactant gives strongly adsorbed product then separated peaks of reactant and products can be collected at the reactor exit [2, 5-8]. Types of reactions and orders of eluted components have a great impact on the reactive chromatography mechanism.

Derivation of analytical solutions are possible for linear chromatographic models. Such solutions are useful for quantifying the effects of mass transfer and reaction rate coefficients on the process [2, 5-7]. For diluted systems, these theoretical results are well applicable. They can also be utilized to verify the results of numerical schemes, to perform sensitivity analysis and to estimate model parameters.

The present work addresses several aspects of fixed bed two-component liquid chromatography, *i. e.* adsorption equilibria and reaction and separation kinetics. It is an extension of our previous work in [7] on reactive chromatography by considering, a part from the solid phase reaction, also the liquid phase reaction. Semi-analytical results are calculated for a linear two-component reactive general rate model (RGRM) considering both liquid and solid phases irreversible reactions. The equations of the model are solved by applying one after another the Laplace transformation and eigen-decomposition technique. The solutions are derived for two types of boundary conditions (BC), known as Dirichlet and Danckwerts types of BC. The Laplace domain solutions are not invertible analytically in to time domain due to the involvement of complicated functions in the solutions. Therefore, a flexible numerical Laplace inversion method of Durbin is utilized for this purpose [12]. A HR-FVS is also applied to the same model equations for validating the semi-analytical solutions [7, 12]. Furthermore, a few case studies are conducted for analyzing the dynamical behavior of the chromatographic reactor.

The mathematical model of irreversible reaction ($M \rightarrow N$)

During the $M \rightarrow N$ type of reaction, the component 1 (the reactant M) is converted into component 2 (the product N) because of an irreversible reaction of first order in both liquid and particle phases.

The bulk phase equations of RGRM are expressed [2, 7]:

$$\frac{\partial c_{m_i}}{\partial t} + u \frac{\partial c_{m_i}}{\partial z} = D_z \frac{\partial^2 c_{m_i}}{\partial z^2} - \frac{3}{R_p} F k_{\text{ext},i} (c_{m_i} - c_{p_m,i} |_{r=R_p}) \mp \mu_1 c_{m_i}, \quad i = 1, 2 \quad (1)$$

Here, t stands for the time and the axial co-ordinate is represented by z . The interstitial velocity is u , the axial dispersion coefficient, D_z , and the external mass transfer coefficient of the i^{th} component is denoted by $k_{\text{ext},i}$. Further, $F = (1 - \epsilon)/\epsilon$ denotes the phase ratio that depends on the total porosity ϵ and μ_1 is the rate constant of first order reaction in the liquid phase.

The mass balance equations in the particles pores are given [2, 7]:

$$\epsilon_p \frac{\partial c_{p_m,i}}{\partial t} + (1-\epsilon_p) \frac{\partial q_{p_m,i}^*}{\partial t} = \frac{1}{r^2} \frac{\partial}{\partial r} \left\{ r^2 \left[\epsilon_p D_{p_m,i} \frac{\partial c_{p_m,i}}{\partial r} + (1-\epsilon_p) D_{s_m,i} \frac{\partial q_{p_m,i}^*}{\partial r} \right] \right\} \mp \mp (1-\epsilon_p) v_1 q_{p_m,i}^*, \quad i = 1, 2 \quad (2)$$

Here, the stationary phase local equilibrium concentration is denoted by $q_{p_m,i}^*$, the internal porosity is expressed by ϵ_p , the i^{th} component pore and surface diffusivities are denoted by $D_{p_m,i}$ and $D_{s_m,i}$, and v_1 is the reaction rate constant in the particle phase.

By using linear adsorption isotherms $q_{p_m,i}^* = a_i c_{p_m,i}$ in eq. (2) [2, 7]:

$$a_i^* \frac{\partial c_{p_m,i}}{\partial t} = \frac{D_{\text{eff},i}}{r^2} \frac{\partial}{\partial r} \left(r^2 \frac{\partial c_{p_m,i}}{\partial r} \right) \mp (1-\epsilon_p) v_1 a_i c_{p_m,i} \quad (3)$$

with

$$a_i^* = \epsilon_p + (1-\epsilon_p) a_i \text{ and } D_{\text{eff},i} = \epsilon_p D_{p_m,i} + (1-\epsilon_p) D_{s_m,i} a_i, \quad i = 1, 2 \quad (4)$$

The following dimensionless variables are used to facilitate our analysis in the next section:

$$\rho^* = \frac{r}{R_p}, \quad x = \frac{z}{l}, \quad \eta_i = \frac{l}{u} \mu_i, \quad \tau = \frac{ut}{l}, \quad \text{Pe}_l = \frac{lu}{D_z}, \quad \omega_i = \frac{l}{u} v_1 a_i \quad (5)$$

$$\text{Bi}_{p_m,i} = \frac{k_{\text{ext},i} R_p}{D_{\text{eff},i}}, \quad \eta_{p_m,i} = \frac{D_{\text{eff},i} l}{R_p^2 u}, \quad \xi_{p_m,i} = 3 \text{Bi}_{p_m,i} \eta_{p_m,i} F, \quad i = 1, 2$$

Here, the column length is denoted by l and the Pectlet number is expressed by symbol Pe_l . By utilizing the aforementioned dimensionless quantities in eqs. (1) and (3):

$$\frac{\partial c_{m_i}}{\partial \tau} + \frac{\partial c_{m_i}}{\partial x} = \frac{1}{\text{Pe}_l} \frac{\partial^2 c_{m_i}}{\partial x^2} - \xi_{p_m,i} (c_{m_i} - c_{p_m,i} |_{\rho^*=1}) \mp \eta_i c_{m_i} \quad (6)$$

$$a_i^* \frac{\partial c_{p_m,i}}{\partial \tau} = \frac{\eta_{p_m,i}}{\rho^{*2}} \frac{\partial}{\partial \rho^*} \left[\left(\rho^{*2} \right) \frac{\partial c_{p_m,i}}{\partial \rho^*} \right] \mp (1-\epsilon_p) \omega_i c_{p_m,i} \quad (7)$$

Rephrasing of eq. (7) provides:

$$a_i^* \frac{\partial}{\partial \tau} [\rho^* c_{p_m,i}] - \eta_{p_m,i} \frac{\partial^2}{\partial \rho^{*2}} [\rho^* c_{p_m,i}] \pm (1-\epsilon_p) \omega_i [\rho c_{p_m,i}] = 0 \quad (8)$$

For an empty column at the beginning, the appropriate initial conditions are expressed:

$$c_{m_i}(t=0, x) = 0, \quad (0 < x < 1), \quad c_{p_m,i}(t=0, x, \rho^*) = 0, \quad x, \rho^* \in (0, 1) \quad (9)$$

Next, we discuss the BC. Either of the two BC can be used to close the aforementioned model equations [2, 7].

Type I: Inlet Dirichlet BC

In this case, simple BC are imposed at the column inlet and outlet for eq. (6):

$$c_{m_i}(\tau, 0) = \begin{cases} c_{i,\text{inj}}, & \text{if } 0 \leq \tau \leq \tau_{\text{inj}} \\ 0, & \tau > \tau_{\text{inj}} \end{cases} \quad (10a)$$

paired with

$$\left. \frac{\partial c_{m_i}}{\partial x} \right|_{x=\infty} = 0 \quad (10b)$$

Type II: Inlet Danckwerts BC

In this case:

$$c_{m_i}(\tau, 0) - \frac{1}{Pe_l} \frac{\partial c_{m_i}(\tau, 0)}{\partial x} = \begin{cases} c_{i, \text{inj}}, & \text{if } 0 \leq \tau \leq \tau_{\text{inj}} \\ 0, & \tau > \tau_{\text{inj}} \end{cases} \quad (11a)$$

While at the column outlet:

$$\left. \frac{\partial c_{m_i}}{\partial x} \right|_{x=1} = 0 \quad (11b)$$

The natural boundary condition at $\rho^* = 0$ and $\rho^* = 1$ are assumed for eq. (8):

$$\left. \frac{\partial c_{p_m, i}}{\partial \rho^*} \right|_{\rho^*=0} = 0, \quad \left. \frac{\partial c_{p_m, i}}{\partial \rho^*} \right|_{\rho^*=1} = Bi_{p_m, i} (c_{m_i} - c_{p_m, i} |_{\rho^*=1}) \quad (12)$$

Derivation of analytical solution

The model eqs. (6) and (8) are solved analytically by utilizing the following Laplace transformation [7]:

$$\bar{c}_{m_i}(s, x) = \int_0^{\infty} e^{-s\tau} c_{m_i}(\tau, x) d\tau, \quad \tau \geq 0 \quad (13)$$

Thus, eq. (6) provides:

$$s\bar{c}_{m_i} + \frac{d\bar{c}_{m_i}}{dx} = \frac{1}{Pe_l} \frac{d^2\bar{c}_{m_i}}{dx^2} - \xi_{p_m, i} (\bar{c}_{m_i} - \bar{c}_{p_m, i} |_{\rho^*=1}) \mp \eta_l \bar{c}_{m_i}, \quad i = 1, 2 \quad (14)$$

While, the Laplace transformations of eq. (8) gives:

$$\frac{d^2}{d\rho^{*2}} [\rho^* \bar{c}_{p_m, i}] - \frac{a_i^* s}{\eta_{p_m, i}} \left[\rho^* \bar{c}_{p_m, i} \right] \pm \frac{(1 - \epsilon_p) \omega_l}{\eta_{p_m, 1}} \left[\rho^* \bar{c}_{p_m, 1} \right] = 0 \quad (15)$$

For $i = 1$, the aforementioned equation has a following solution:

$$\bar{c}_{p_m, 1}(s, x, \rho^*) = \frac{[K_1 e^{\sqrt{\alpha_m(s)} \rho^*} + K_2 e^{-\sqrt{\alpha_m(s)} \rho^*}]}{\rho^*} \quad (16)$$

where

$$\alpha_m(s) = \frac{sa_1^* + (1 - \epsilon_p) \omega_l}{\eta_{p_m, 1}}$$

and the values of constant K_1 and K_2 in eq. (16) are evaluated by using the BC given by eq. (12):

$$K_{1,2} = \pm \frac{Bi_{p_m, 1} \bar{c}_{m_i}}{2 \sinh \left[\sqrt{\alpha_m(s)} \right] \left[\sqrt{\alpha_m(s)} \coth \left(\sqrt{\alpha_m(s)} + Bi_{p_m, 1} - 1 \right) \right]} \quad (17)$$

Here, for K_1 positive symbol is used and for K_2 negative symbol is used. Equations (16) and (17) for the value of $\rho^* = 1$ are reduced:

$$\bar{c}_{p_m,1} \Big|_{\rho^*=1} = \bar{c}_{m_1} f_1(s) \quad (18)$$

where

$$f_1(s) = \frac{\text{Bi}_{p_m,1}}{\left[-1 + \sqrt{\alpha_m(s)} \coth\left(\sqrt{\alpha_m(s)}\right) + \text{Bi}_{p_m,1} \right]} \quad (19)$$

For $i = 2$ and using eq. (18), the solution of eq. (15):

$$\bar{c}_{p_m,2}(s, x, \rho^*) = \frac{\left[K'_1 e^{\sqrt{\alpha'_m(s)} \rho^*} + K'_2 e^{-\sqrt{\alpha'_m(s)} \rho^*} \right]}{\rho^*} + \frac{(1 - \epsilon_p) f_1(s) \omega_1 \bar{c}_{m_1} \sinh\left(\sqrt{\alpha_m(s)} \rho^*\right)}{\rho^* \left(\alpha_m(s) \eta_{p_m,2} - a_2^* s \right) \sinh\left(\sqrt{\alpha_m(s)}\right)} \quad (20)$$

where

$$\alpha'_m(s) = \frac{a_2^* s}{\eta_{p_m,2}}$$

Using eq. (12) in eq. (20):

$$K'_{1,2} = \pm \frac{\text{Bi}_{p_m,2} \bar{c}_{m_2} - \frac{(1 - \text{Bi}_{p_m,2}) f_1(s) (1 - \epsilon_p) \omega_1 \bar{c}_{m_1}}{2(\alpha(s) \eta_{p_m,2} - a_2^* s)}}{2 \sinh\left(\sqrt{\alpha'_m(s)}\right) \left[-1 + \sqrt{\alpha'_m(s)} \coth\left(\sqrt{\alpha'_m(s)}\right) + \text{Bi}_{p_m,2} \right]} \quad (21)$$

For $\rho^* = 1$, the eqs. (20) and (21) are simplified:

$$\bar{c}_{p_m,2} \Big|_{\rho^*=1} = \bar{c}_{m_2} f_2(s) + \bar{c}_{m_1} A_m(s) \quad (22)$$

where

$$f_2(s) = \frac{\text{Bi}_{p_m,2}}{\left[\sqrt{\alpha'_m(s)} \coth\left(\sqrt{\alpha'_m(s)}\right) + \text{Bi}_{p_m,2} - 1 \right]} \quad (23)$$

and

$$A_m(s) = \frac{f_1(s) (1 - \epsilon_p) \omega_1}{\alpha_m(s) \eta_{p_m,2} - a_2^* s} \left[\frac{(\text{Bi}_{p_m,2} - 1)}{\left[\sqrt{\alpha'_m(s)} \coth\left(\sqrt{\alpha'_m(s)}\right) + \text{Bi}_{p_m,2} - 1 \right]} - 1 \right] \quad (24)$$

After introducing eqs. (18) and (22) in eq. (14) the following pair of ODE are obtained:

$$\frac{d^2 \bar{c}_{m_1}}{dx^2} - \text{Pe}_l \frac{d\bar{c}_{m_1}}{dx} - \text{Pe}_l \phi_{m_1}(s) \bar{c}_{m_1} = \text{Pe}_l \eta_1 \bar{c}_{m_1} \quad (25)$$

$$\frac{d^2 \bar{c}_{m_2}}{dx^2} - \text{Pe}_l \frac{d\bar{c}_{m_2}}{dx} - \text{Pe}_l \phi_{m_2}(s) \bar{c}_{m_2} = \text{Pe}_l \left(\eta_1 - \xi_{p_m,2} A_m(s) \right) \bar{c}_{m_1} \quad (26)$$

where

$$\phi_{m_1}(s) = s + \xi_{p_m,1}(1 - f_1(s)), \quad \phi_{m_2}(s) = s + \xi_{p_m,2}(1 - f_2(s)) \quad (27)$$

In matrix representation, eqs. (25) and (26) are given:

$$\frac{d^2}{dx^2} \begin{pmatrix} \bar{c}_{m_1} \\ \bar{c}_{m_2} \end{pmatrix} - \text{Pe}_l \frac{d}{dx} \begin{pmatrix} \bar{c}_{m_1} \\ \bar{c}_{m_2} \end{pmatrix} - \begin{bmatrix} \text{Pe}_l \phi_{m_1}(s) + \text{Pe}_l \eta_1 & 0 \\ \text{Pe}_l \eta_1 - \xi_{p_m,2} \text{Pe}_l A(s) & \text{Pe}_l \phi_{m_2}(s) \end{bmatrix} \begin{pmatrix} \bar{c}_{m_1} \\ \bar{c}_{m_2} \end{pmatrix} = \begin{pmatrix} 0 \\ 0 \end{pmatrix} \quad (28)$$

Here, \bar{c}_{m_i} expresses the Laplace domain concentrations.

The value of $[B]$ in eq. (28) is given:

$$B = \begin{bmatrix} \text{Pe}_l \phi_{m_1}(s) + \text{Pe}_l \eta_1 & 0 \\ \text{Pe}_l \eta_1 - \xi_{p_m,2} \text{Pe}_l A_m(s) & \text{Pe}_l \phi_{m_2}(s) \end{bmatrix} \quad (29)$$

The eigenvalues λ_1^* and λ_2^* and the eigenvectors A_{11} and A_{22} for the aforementioned matrix are expressed:

$$\lambda_1^* = \text{Pe}_l \phi_{m_1}(s) + \text{Pe}_l \eta_1, \quad x_1 = \begin{pmatrix} A_{11} \\ \frac{\text{Pe}_l \eta_1 - \xi_{p_m,2} \text{Pe}_l A_m(s) A_{11}}{\text{Pe}_l \phi_{m_1}(s) - \text{Pe}_l \phi_{m_2}(s) + \text{Pe}_l \eta_1} \end{pmatrix}, \quad \lambda_2^* = \text{Pe}_l \phi_{m_2}(s), \quad x_2 = \begin{pmatrix} 0 \\ A_{22} \end{pmatrix} \quad (30)$$

For the sake of simplicity, we have selected A_{11} and A_{22} equal to one:

$$\kappa = \begin{bmatrix} \text{Pe}_l \phi_{m_1}(s) + \text{Pe}_l \eta_1 & 0 \\ 0 & \text{Pe}_l \phi_{m_2}(s) \end{bmatrix}, \quad A = \begin{bmatrix} 1 & 0 \\ \frac{\text{Pe}_l \eta_1 - \xi_{p_m,2} \text{Pe}_l A_m(s)}{\text{Pe}_l \phi_{m_1}(s) - \text{Pe}_l \phi_{m_2}(s) + \text{Pe}_l \eta_1} & 1 \end{bmatrix} \quad (31)$$

The linear transformation by using the previous matrix $[A]$ can be written:

$$\begin{pmatrix} \bar{c}_{m_1} \\ \bar{c}_{m_2} \end{pmatrix} = \begin{bmatrix} 1 & 0 \\ \frac{\text{Pe}_l \eta_1 - \xi_{p_m,2} \text{Pe}_l A(s)}{\text{Pe}_l \phi_{m_1}(s) - \text{Pe}_l \phi_{m_2}(s) + \text{Pe}_l \eta_1} & 1 \end{bmatrix} \begin{pmatrix} b_1 \\ b_2 \end{pmatrix} \quad (32)$$

Using aforementioned linear transformation in eq. (28):

$$\frac{d^2}{dx^2} \begin{pmatrix} b_1 \\ b_2 \end{pmatrix} - \text{Pe}_l \frac{d}{dx} \begin{pmatrix} b_1 \\ b_2 \end{pmatrix} = \begin{bmatrix} \text{Pe}_l \phi_{m_1}(s) + \text{Pe}_l \eta_1 & 0 \\ 0 & \text{Pe}_l \phi_{m_2}(s) \end{bmatrix} \begin{pmatrix} b_1 \\ b_2 \end{pmatrix} \quad (33)$$

Equation (33) shows a pair of two ODE whose solutions are represented:

$$b_1(s, x) = A_1 e^{D_1 x} + B_1 e^{D_2 x}, \quad D_{1,2} = \frac{\text{Pe}_l}{2} \left(1 \mp \sqrt{1 + \frac{4\phi_{m_1}(s) + \text{Pe}_l \eta_1}{\text{Pe}_l}} \right) \quad (34)$$

and

$$b_2(s, x) = A_2 e^{D^3 x} + B_2 e^{D^4 x}, \quad D_{3,4} = \frac{\text{Pe}}{2} \left(1 \pm \sqrt{1 + \frac{(\quad)}{\text{Pe}}} \right) \quad (35)$$

Here, the values of the constant are derived by using two sets of boundary conditions.

Type I: Inlet Dirichlet BC

In the Laplace domain eqs. (10a) and (10b) are represented:

$$\bar{c}_{m_i}(s, 0) = \left(1 - e^{-s\tau_{inj}}\right) \frac{c_{i, inj}}{s}, \quad \frac{d\bar{c}_{m_i}}{dx}(s, \infty) = 0 \quad (36)$$

On utilizing eq. (32), eq. (36) yields:

$$b_1(s, 0) = \frac{\left(1 - e^{-s\tau_{inj}}\right)}{s} c_{1, inj}, \quad \frac{db_1}{dx}(s, \infty) = 0 \quad (37)$$

$$b_2(s, 0) = \frac{\left(1 - e^{-s\tau_{inj}}\right)}{s} c_{2, inj} - \frac{\left(\eta_1 - \xi_{p, 2} Pe_l A(s)\right)}{Pe_l (\phi_1(s) - \phi_2(s)) + \eta_1} b_1(s, 0), \quad \frac{db_2}{dx}(s, \infty) = 0 \quad (38)$$

On using previous equations, the constants are expressed:

$$A_1 = \left(1 - e^{-s\tau_{inj}}\right) \frac{c_{1, inj}}{s}, \quad B_1 = 0 \quad (39)$$

$$A_2 = \frac{\left(1 - e^{-s\tau_{inj}}\right)}{s} \left[c_{2, inj} - \frac{\left(\eta_1 - \xi_{p, 2} Pe_l A(s)\right)}{Pe_l (\phi_1(s) - \phi_2(s)) + \eta_1} c_{1, inj} \right], \quad B_2 = 0 \quad (40)$$

Thus, eqs. (32), (34), and (35) together with previous equations give:

$$\bar{c}_{m_i}(s, x) = \frac{c_{inj, i} \left(1 - e^{-s\tau_{inj}}\right)}{s} e^{D_1 x} \quad (41)$$

and

$$\bar{c}_{m_2}(s, x) = \left(1 - e^{-s\tau_{inj}}\right) \frac{c_{1, inj}}{s} \left(\frac{\left(\eta_1 - \xi_{p, 2} A(s)\right)}{Pe_l (\phi_1(s) - \phi_2(s)) + \eta_1} \right) \left(e^{D_1 x} - e^{D_3 x} \right) + \left(1 - e^{-s\tau_{inj}}\right) \frac{c_{2, inj}}{s} e^{D_3 x} \quad (42)$$

Type II: Inlet Danckwerts BC

Equations (11a) and (11b) in the Laplace domain are given:

$$\bar{c}_{m_i}(s, 0) = \frac{c_{i, inj} \left(1 - e^{-s\tau_{inj}}\right)}{s} + \frac{1}{Pe_l} \frac{d\bar{c}_i}{dx} \Big|_{x=0}, \quad \frac{d\bar{c}_i}{dx}(s, 1) = 0, \quad i = 1, 2 \quad (43)$$

Repeating the solution methodology discussed in previous subsection, the Laplace domain solutions are represented:

$$\bar{c}_{m_i}(s, x) = \frac{c_{1, inj} \left(1 - e^{-s\tau_{inj}}\right)}{s} \frac{\left(D_2 - D_1\right) e^{D_2 + D_1}}{\left(1 - \frac{m_1}{Pe_l}\right) D_2 e^{D_2} - \left(1 - \frac{D_2}{Pe_l}\right) D_1 e^{D_1}} \quad (44)$$

$$\bar{c}_{m_2}(s, x) = \frac{(-\eta_1 - \xi_{p,2}A(s))}{(Pe_l\phi_1(s) + \eta_1 - Pe_l\phi_2(s))} \frac{c_{1,inj}(1 - e^{-s\tau_{inj}})}{s} \frac{(D_2 - D_1)e^{D_2+D_1}}{\left(1 - \frac{D_1}{Pe_l}\right)D_2e^{D_2} - \left(1 - \frac{D_2}{Pe_l}\right)D_1e^{D_1}} +$$

$$+ \frac{(1 - e^{-s\tau_{inj}})}{s} \left[c_{2,inj} - \left(\frac{(-\eta_1 - \xi_{p,2}FA(s))}{(Pe_l\phi_1(s) + \eta_1 - Pe_l\phi_2(s))} \right) c_{1,inj} \right] \frac{(D_3 - D_4)e^{(D_4+D_3)}}{\left(1 - \frac{D_4}{Pe_l}\right)D_3e^{D_3} - \left(1 - \frac{D_3}{Pe_l}\right)D_4e^{D_4}} \quad (45)$$

For small axial dispersion for example $D \leq 10^{-5}$ cm² per minute, the Danckwert boundary conditions simply reduce to the Dirichlet boundary conditions. Inverse Laplace transform is not possible analytically due to the involvement of complicated functions in the solutions. Therefore, In order to get the aforementioned solutions in the time domain, the numerical Laplace inversion is implemented. An accurate and efficient Fourier series based algorithm is used in this work [10].

Numerical case studies

In this section, several test problems are conducted for showing the effects of model parameters on the process, such as axial Peclet number, Pe_l , film mass transfer resistance, Bi_p , intraparticle diffusion resistance, η_p , solid phase reaction rate constant, ω_1 , and liquid phase reaction rate constant, η_1 . The value of standard parameters used in this work are listed in tab. 1.

Table 1. Parameters of linear two-component RGRM, here $i = 2$

Parameters	L [cm]	ϵ [-]	u [cmmin ⁻¹]	D_z [cm ² min ⁻¹]	$D_{eff,m,i}$ [cm ² min ⁻¹]	t_{max} [min]	$c_{i,inj}$ [g l ⁻¹]	a_1 [-]	a_2 [-]	ω [-]	η_1 [-]
Values	10	0.4	2.5	0.34	0.0001	50	0.5	2.5	0.5	0.2	0.2

In fig. 1, the concentration of both components (reactant and product) are examined by varying the volume of injected sample. A finite width rectangular pulse is injected at the inlet of the empty column. The concentration profiles of component 1 and component 2 are plotted at the outlet of the column (*i. e.* at $x = 1$). In fig. 1(a), when the same quantity of both components are used in the injection, more amount of the product is achieved because of the irreversibility of reaction. Whereas, in fig. 1(b), the half amount of product is injected ($c_{inj,1} = 0.25$ g/l) as compared to the component 1 ($c_{inj,1} = 0.5$ g/l). The conversion of reactant is the same but due to the small amount of injected volume of the product, a small height of component 2 is observed at the column outlet. Moreover, residence time of component 1 in the column is greater due to its larger affinity as compared to component 2 ($a_1 = 2.5$ and $a_2 = 0.5$). Good agreement between semi-analytical and numerical solutions are observed in both the cases.

Figure 2 gives the plots of elution profiles for components 1 and 2 by varying solid phase reaction rate constant, ω_1 , and keeping fixed the liquid phase reaction rate, $\eta_1 = 0.2$. It is noticed that product is increasing on increasing the value of solid phase reaction rate constant.

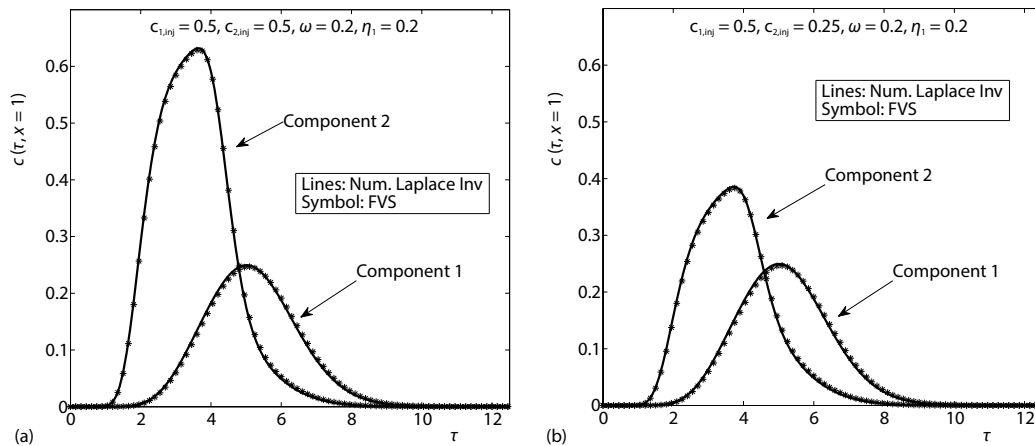


Figure 1. Effect of the injection volume on the outlet concentration profiles (*i. e.* at $x = 1$) obtained by Dirichlet BC

Figure 3 explains the different effects of Dirichlet and Danckwert boundary conditions on the eluted components. The eluted components are examined for three values of Pe_l taking $\omega_1 = 0.2$ and $\eta_1 = 0.2$. It is clear from the plots that for a small Peclet number (or larger radial dispersion coefficient), the concentration profiles for Dirichlet and Danckwert BC are deviating from each other. Whereas, for larger Peclet numbers ($Pe_l = 125$ and $Pe_l = 225$) (or for small axial dispersion coefficients), the eluted profiles are almost identical for both BC. For that reason, the more accurate Danckwerts BC are always recommended for larger axial dispersion coefficients (smaller Peclet numbers) to account for the mass loss due to back mixing near the column entrance.

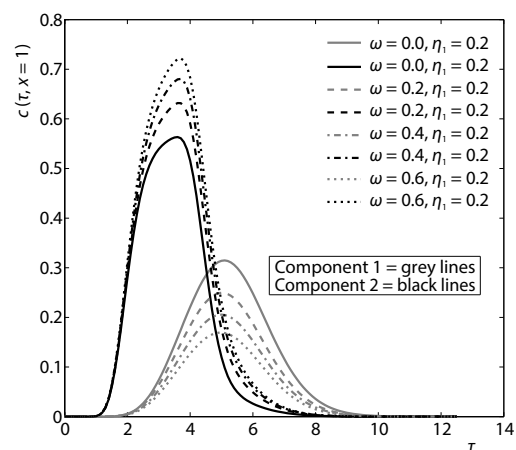


Figure 2. Effect of the solid phase reaction rate constant ω on the concentration profiles at $x = 1$ using Danckwert BC

Figure 4 depicts the effects of liquid phase reaction rate constant, η_1 , on the concentration profiles for a fixed value of solid phase reaction rate constant, $\omega_1 = 0.2$. Here, we have chosen the same parameters given in the tab. 1. Same behaviors of reactant and product are observed in this case.

Figure 5(a) explains the effect of Biot number, Bi_{pm} on the concentration profiles. Broadened peaks of profiles are observed for $Bi_p = 50$, whereas $Bi_p = 0.5$ has generated steeped profiles. Figure 5(b) shows the intraparticle diffusion effect on the profiles. Plots are obtained for fixed value of Pe_l and varying the value of η_p . It is clearly observed that for a slow diffusion rate $\eta_p = 0.02$, the residence time inside the column decreases for both the components. Whereas, larger value $\eta_p = 20$ gives an increased retention time. Moreover, an increase of η_p also increases separation of the components.

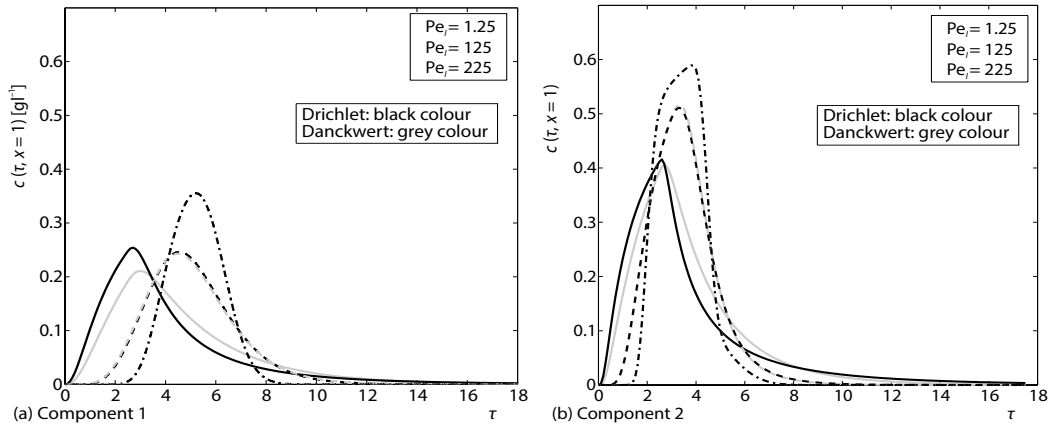


Figure 3. Effects of the Dirichlet and Danckwert BC on the concentration profiles at $x = 1$, with $c_{1,inj} = 0.5$ g/l and $c_{2,inj} = 0.5$ g/l (for color image see journal web site)

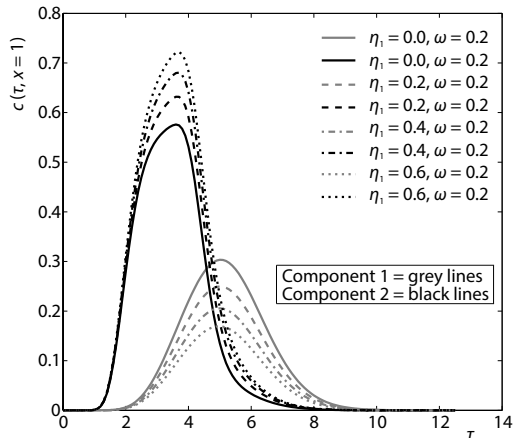


Figure 4. Effect of the liquid phase reaction rate constant η_p on the concentration profiles at $x = 1$ using Danckwert BC (for color image see journal web site)

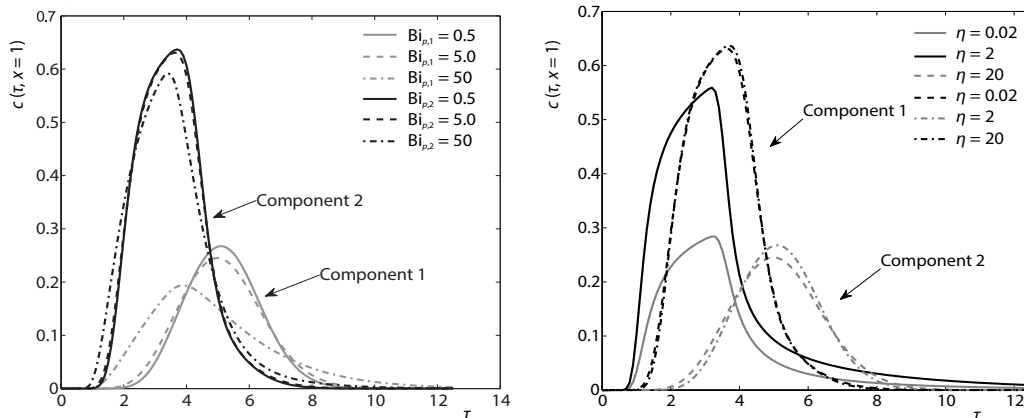


Figure 5: Effect of $Bi_{p,i}$ and η_p on the concentration profiles for Danckwert BC

Conclusion

A two-component general rate model was solved analytically to simulate separation and reaction processes inside the chromatographic reactor. The desired semi-analytical results were obtained by applying one after another the Laplace transformation and the eigen decomposition method. The solutions were obtained for irreversible reaction and for two sets of boundary conditions. An efficient and flexible numerical Laplace inversion technique was used to retrieve back solutions in the time domain. The second order HR-FVS was used for the comparison of the results [12, 13]. A good agreement between numerical and analytical results verified the accuracy of the

numerical scheme and the correctness of derived analytical results. Selected parametric studies for liquid and solid phase reaction rate constants, intraparticle diffusion resistance, film mass transfer resistance and axial dispersion were performed. It was found that conversion of the reactants into product increases on increasing the reaction rates in both phases. The derived analytical results are useful tools for further improvements in the performance of chromatographic reactors.

Nomenclature

a_i – Henry's constant for component i , [-]
 $c_{i,\text{inj}}$ – injected concentration, [g l^{-1}]
 c_{mi} – liquid concentration in the bulk, [g l^{-1}]
 $c_{pm,i}$ – liquid concentration in the pores, [g l^{-1}]
 $D_{\text{eff},m,i}$ – effective dispersion coefficient, [cm $^2\text{min}^{-1}$]
 $D_{pm,i}$ – pore diffusivity coefficient, [cm $^2\text{min}^{-1}$]
 $D_{s,m,i}$ – surface diffusivity coefficient, [cm $^2\text{min}^{-1}$]
 D_z – axial dispersion coefficient, [cm $^2\text{min}^{-1}$]
 $q_{pm,i}^*$ – solid phase concentration, [g l^{-1}]
 r – particle radial co-ordinate, [min]

t – time co-ordinate, [min]
 u – interstitial phase velocity, [cm min^{-1}]
 t_{inj} – time of injection, [-]
 t_{max} – total simulation time, [min]

Greek symbols

ϵ – total porosity, [-]
 η_i – liquid phase reaction rate, [-]
 ω – solid phase reaction rate, [-]

References

- [1] Ganetsos, G., Barker, P. E., *Preparative and Production Scale Chromatography*, Marcel Dekker, Inc., New York, USA, Vol. 61, pp. 375-523, 1993
- [2] Guiochon, G., *et al.*, *Fundamentals of Preparative and Non-Linear Chromatography*, 2nd ed., Elsevier, Inc., Amsterdam, The Netherlands, 2006
- [3] Wang, C.-C., Yau, H. -T., Application of Hybrid Microwave Thermal Extraction Techniques for Mulberry Root Bark, *Thermal Science*, 17 (2013), 5, pp. 1311-1315
- [4] Adiguzel, A. C., *et al.*, Determination of Glass Transition Temperature and Surface Properties of Novel Chalcone Modified Poly (Styrene) Based Polymer, *Thermal Science*, 23 (2019), Suppl. 1, pp. S193-S202
- [5] Qamar, S., *et al.*, Irreversible and Reversible Reactions in a Liquid Chromatographic Column: Analytical Solutions and Moment Analysis, *Ind. Eng. Chem. Res.*, 53 (2014), 6, pp. 2461-2472
- [6] Bibi, S., *et al.*, Irreversible and Reversible Reactive Chromatography: Analytical Solutions and Moment Analysis for Rectangular Pulse Injections, *Journal Chromatogr. A* 1385 (2015), Mar., pp. 49-62
- [7] Bashir, S., *et al.*, Analysis of Linear Reactive General Rate Model of Liquid Chromatography Considering Irreversible and Reversible Reactions, *Chem. Eng. Res. Design*, 119 (2017), Mar., pp. 140-159
- [8] Schweich, D., Villermaux, J., The Chromatographic Reactor, A New Theoretical Approach, *Ind. Eng. Chem. Fundamen*, 17 (1978), pp. 1-7
- [9] Fricke, J., *et al.*, *Chromatographic Reactor*, Ullmann's Encyclopedia of Industrial Chemistry, Wiley-VCH Verlag, Weinheim, 2005
- [10] Sardin, M., *et al.*, (Eds.), *Preparative Fixed-Bed Chromatographic Reactor; Preparative and Production Scale Chromatography*, Marcel Dekker Inc., New York, USA, pp. 477, 1993
- [11] Villermaux, J., *et al.*, (Eds.), The Chromatographic Reactor in Percolation Processes, in: *Theory and Applications*, Sijthoff Noordhoff, Alpena an den Rijn, The Netherlands, pp. 539-588, 1981
- [12] Durbin, F., Numerical Inversion of Laplace Transforms: An Efficient Improvement to Dubner and Abate's Method, *Comput. J.*, 17 (1974), pp. 371-376
- [13] Koren, B., *A Robust Upwind Discretization Method for Advection, Diffusion and Source Terms*, (Ed. C. B. Vreugdenhil, B. Koren), Numerical Methods for Advection-Diffusion Problems, Notes on Numerical Fluid Mechanics, Chapter 5, Vol. 45, pp. 117-138, Vieweg Verlag, Braunschweig, 1993